

**UV-IR Spectra of the New Tellurite Glasses of  
The System  $\text{TeO}_2$  - $\text{La}_2\text{O}_3$  and  $\text{TeO}_2$  - $\text{V}_2\text{O}_5$**

**R.El-Mallawany, A.Abdel-Kader, M.El-Hawary and N.El-Khoshkhany**

Physics Dept., Faculty of Science, Menofia Univ., EGYPT.

**Abstract:**

Binary tellurite glass systems of the forms  $(\text{TeO}_2)_{(100-x)}-(\text{A}_n\text{O}_m)_x$  where  $\text{A}_n\text{O}_m = \text{La}_2\text{O}_3$  or  $\text{V}_2\text{O}_5$  and  $x = 5$  to  $20$  for  $\text{La}_2\text{O}_3$  and  $10$  to  $50$  for  $\text{V}_2\text{O}_5$  were prepared. UV- spectra of these glasses were recorded in the range of  $200$ - $600$  nm at room temperature. The optical energy gaps  $E_{\text{optical}}$  and  $E_{\text{tail}}$  have been calculated from the optical absorption edge. UV cut-off and IR cut-off have been measured. Calculations of the oxide ion average Polarizability ( $\alpha_0^{2-}$ ) and optical basicity ( $\Lambda$ ) have been done.

**1- Introduction:**

Tellurite glasses are of scientific and technological interest because of their high refractive indices, low melting temperatures, high dielectric constants as well as their good UV and IR transmissions and considered as promising materials for non- linear optical devices as explained. Some tellurite glasses are also reported to be suitable for setting up optical fiber amplifiers [1]. The absorption edge of each glass depends on the type of network modifier. The absorption coefficient,  $\alpha(\omega)$ , can be determined near the absorption edge using the formula:

$$\alpha(\omega) = \left(\frac{1}{d}\right) \ln\left(\frac{I_0}{I}\right) \quad (1)$$

where  $d$  is the thickness of the sample,  $I_0$ ,  $I$  are the intensities of the incident and transmitted beams respectively. For many oxide glasses and other amorphous materials, Urbach rule [2] has been applied.

$$\alpha(\omega) = \alpha_0 \exp(\hbar\omega / E_t) \quad (2)$$

angular frequency and  $E_t$  is the Urbach energy which is interpreted as the width of the tails of the localized states in the band gap associated with the amorphous nature of the material. When the density of states is proportional to some power of

R. EL – Malawany et al .

energy  $(\alpha\hbar\omega)^{1/2}$  and the relation between absorption coefficient and photon energy gap is considered [3,4], this relation can be re-written as follows :

$$(\alpha\hbar\omega)^{1/2} = A(\hbar\omega - E_{opt}) \quad (3)$$

Where A is a constant and  $E_{opt}$  is the optical band gap determined by extra polating the linear parts of the curves to  $(\alpha\hbar\omega)^{1/2} = 0$ .

## **2- Experimental procedure:**

Binary tellurite glass systems of the forms  $(TeO_2)_{(100-x)}-(A_nO_m)_x$  where  $A_nO_m = La_2O_3$  or  $V_2O_5$  and  $x = 5$  to 20 for  $La_2O_3$  and 10 to 50 for  $V_2O_5$  were prepared as described in part 1 of this work Ref.(5).

### **2.1. Ultraviolet absorption spectra measurements (UV):**

The UV absorption measurements for the bulk glass samples with the two parallel polished faces were measured using a UV-spectrophotometer (Perkin-Elmer Lambda 4B) in the wavelength range 200-600nm at room temperature.

### **2.2. Infrared absorption spectra measurements (IR):**

The IR absorption spectra of the prepared glasses in KBr matrix were recorded on a Perkin-Elmer double beam spectrophotometer model 598 at room temperature over the spectral range of 4000-200  $cm^{-1}$ . The produced glasses were thoroughly mixed with KBr in the ratio 1:40, after that the mixtures were pressed at 10 tons for 5 min.. The pellets were clear and uniform. While recording the spectra, the gain of the spectrometer was kept the same for all the samples.

## **3- Results and Discussion:**

### **3-1 U.V of Tellurite glasses:**

Optical absorption measurements in the spectral range 200-600 nm were made at room temperature for the glass samples of the composition of  $(TeO_2)_{(100-x)}-(La_2O_3)_x$  where  $[x = 5, 7.5, 10, 12.5, 15, 17.5$  and 20 mol%] and  $(TeO_2)_{(100-x)}-(V_2O_5)_x$  where  $[x = 10, 20, 25, 30, 35, 40, 45$  and 50 mol%]. The ultraviolet light absorbance of the prepared tellurite glasses containing  $La_2O_3$  and  $V_2O_5$  as a function wavelength are shown in Fig.(1-a&b) respectively. The absorption edge of each glass can be identified. There are no sharp absorption edges and this is

characteristic of most glassy oxide materials. It is shown in Fig.(1-a&b) that the absorption edge depends on the kind of the modifier. The position of the fundamental absorption edge shifts to lower wavelength with increasing of  $\text{La}_2\text{O}_3$  content in binary  $\text{TeO}_2$ - $\text{La}_2\text{O}_3$  glass or increasing of  $\text{V}_2\text{O}_5$  content in binary  $\text{TeO}_2$ - $\text{V}_2\text{O}_5$  glass. The shifts of the absorption edge are most likely related to the structural rearrangement of the glass and the relative concentrations of the various fundamental units.

The absorption coefficient  $\alpha(\omega)$  can be determined near the absorption edge from the formula (1). The most satisfactory results were obtained by plotting the quantity  $(\alpha\hbar\omega)^{1/2}$  as a function of  $(\hbar\omega)$  as suggested by Davis and Mott [3] as shown by Eq.(3). Absorption by indirect transitions applies to many oxide glasses, particularly at the higher values of absorption coefficient.  $\hbar$  is the reduced Planck's constant and  $\omega$  is the angular frequency of the incident radiation. Fig.(2-a&b) show the plots of  $(\alpha\hbar\omega)^{1/2}$  against  $(\hbar\omega)$  and the values of  $E_{\text{opt}}$  determined by extrapolating the linear parts of the curves to  $(\alpha\hbar\omega)^{1/2}=0$ . The value of  $E_{\text{opt}}$  for each glass system are given in Table (1) and represented in Fig.(3-a&b) as a function of  $\text{La}_2\text{O}_3$  mol% and  $\text{V}_2\text{O}_5$  mol% respectively. From Fig.(3-a) it is clear that the value of  $E_{\text{opt}}$  increases from (3.51 to 3.61eV) due to the modification of tellurite glasses by (5 to 20) mol%  $\text{La}_2\text{O}_3$ . The values of the constant A in Eq.(3) can be determined from the slope of the linear part of the relation  $(\alpha\hbar\omega)^{1/2}$  and  $\hbar\omega$  which is change from (5.38 to 4.8  $\text{cm}^{-1}\text{eV}^{-1}$ ) due to the modification of tellurite glasses by (5 to 20) mol%  $\text{La}_2\text{O}_3$ . From Fig.(3-b) it is clear that the value of  $E_{\text{opt}}$  increase from (2.67 to 3.03eV) due to the modification of tellurite glasses by (10 to 50) mol%  $\text{V}_2\text{O}_5$ . The values of the constant A in Eq.(3) can be determined from the slope of the linear part of the relation  $(\alpha\hbar\omega)^{1/2}$  and  $\hbar\omega$  which is change from (3.04 to 3.38  $\text{cm}^{-1}\text{eV}^{-1}$ ) due to the modification of tellurite glasses by (10 to 50) mol%  $\text{V}_2\text{O}_5$ . Those values are of the same order as reported by Davis & Mott [3]. The interpretation of the present optical energy gap will be based on the assumption that tellurite glasses having a high concentration of  $\text{TeO}_2$ , the triangular bipyramid  $\text{TeO}_4$  is considered

R. EL – Malawany et al .

as the basic co-ordination polyhedron in which tellurium atoms are surrounded by four oxygen and each oxygen is connected with two tellurium atoms, accomplishing an axial-equatorial bonding at which the bonds are easily deformed because of the change in the  $Te_{ax}-O_{eq}-Te$  angle taken place along the c-axis due to the structural incorporation of the modifier which creates defects, oxygen vacancies and microholes, and also increases the concentration of non-bridging oxygen [6]. The doping with transition metal oxides decrease the  $E_{opt}$  of  $(TeO_2)$  which was 3.79 eV [7 ] to the values mentioned before and can be attributed to the increase of the non-bridging oxygen atoms. While doping with  $La_2O_3$  gave a lower concentration of non-bridging oxygen atoms than  $V_2O_5$ . The estimated value of  $E_{opt}$  for  $La_2O_3$  tellurite glasses are close to the reported values in [8]. For many amorphous materials, Urbach [2] assumed that the absorption coefficient  $\alpha(\omega)$  was an exponential function of photon energy  $\hbar\omega$  as shown by Eq.(2). Fig.(4-a&b ) show the variation of  $\ln(\alpha)$  against  $\hbar\omega$  for the present binary glassy systems. The values of  $E_{ta}$  in Eq.(2) are calculated from the slopes of the linear regions of those curves. The values of  $E_{ta}$  for each glasses system are given in Table (1). It is clear that the values of  $E_{ta}$  decrease from (0.1006 to 0.0826 eV) due to the modification of tellurite glasses by (5 to 20) mol%  $La_2O_3$  and from (0.2085 to 0.1619 eV) due to the modification of tellurite glasses by (10 to 50) mol%  $V_2O_5$ . These values are in the range of amorphous semiconductors between 0.046 and 0.66 eV were reported by Davis& Mott [3]. It is clear from these values that the widths of the band tails of the localized states are found to depend upon the kind of the modifier.

Now in the present study, we calculate the electronic polarizability and optical basicity values by using average electronegativity ( $\chi_{2av}$ ) for binary oxide glasses  $TeO_2-La_2O_3$  and  $TeO_2-V_2O_5$  by using Eqs.(4 ,5, 6) which have been stated by Reddy et al [9] as follows

$$(\chi_{2av}) = \frac{X_{xf} + Y_{xs}}{X + Y} \quad (4)$$

$$\alpha_0^{2-} = 3.319 - 0.3422x_{2av} \quad (5)$$

$$\Lambda = 0.04375 + 0.3097 x_{2av} \quad (6)$$

The results are listed in Table (2). We notice that, the electronic polarizability and optical basicity values of  $V_2O_5$ - $TeO_2$  equal the same values of the electronic polarizability and optical basicity of  $V_2O_5$ - $GeO_2$ . The optical basicity of  $V_2O_5$ - $TeO_2$  show large oxide ion polarizability between 2-3 Å. These results are closed with Reddy et al [9] results.

### 3.3. IR of Tellurite Glass:

The room temperature IR spectra in the region 200-4000  $cm^{-1}$  of tellurite glasses containing (5 to 20) mol%  $La_2O_3$  are shown in Fig. (5-a) and for more details Fig.(5-b) represents the IR spectra in the range 200 - 1000  $cm^{-1}$ . The major absorption of glasses at different composition is summarized in Table (3). The region below 300 $cm^{-1}$  for all samples did not show any sensitivity, possibly due to excessive noise and hence this region has been excluded from the discussion. No water bond or —OH stretching modes are observed in the IR spectra of the crystalline  $TeO_2$ . But the binary samples exhibited a water band at 3400  $cm^{-1}$  and an —OH stretching at 2920  $cm^{-1}$ . The main absorption bands are at frequencies around 610-670  $cm^{-1}$ , a shoulder at 580-630  $cm^{-1}$ , a small bands at 560-610  $cm^{-1}$  and a shoulder at 750-780  $cm^{-1}$  posses deformed  $TeO_4$  groups as mentioned by Y.Dimitriev [10]. A new shoulder at 580-630  $cm^{-1}$  was attributed to La-O stretching vibration as measured by A.A.Bahgat [11]. A small band is observed in the spectra at 560-610  $cm^{-1}$ , which may be attributed to Te-O bond vibrations, where the oxygen anions are considered non-bridging (NBO) as measured by E.E.Shaisha [12].

By analogy with the crystalline tellurite [13] it may be accepted that with the introduction of other oxides in tellurite glasses, part of the  $TeO_4$  groups are transformed into  $TeO_3$ . Tellurite containing  $TeO_4$  groups have four band  $v_{eq}^s$ ,  $v_{ax}^{ax}$ ,  $v_{ax}^{ax}$  and  $v_{ax}^s$  modes and the stretching frequencies in the following manner as stated by [14]:

R. EL – Malawany et al .

$$\begin{aligned} \nu_{\text{eq}}^{\text{s}}(\text{TeO}_2) &= 780 \text{ cm}^{-1} & \nu_{\text{ax}}^{\text{ax}}(\text{TeO}_2) &= 675 \text{ cm}^{-1}, \\ \nu_{\text{eq}}^{\text{ax}}(\text{TeO}_2) &= 714 \text{ cm}^{-1} & \nu_{\text{ax}}^{\text{s}}(\text{TeO}_2) &= 635 \text{ cm}^{-1}. \end{aligned}$$

The infrared spectra in the region 200-4000  $\text{cm}^{-1}$  of tellurite glasses containing (10 – 50) mol%  $\text{V}_2\text{O}_5$  are shown in Fig.(6-a), and for more details Fig.(6-b) represents the IR spectra in the range 200-1000  $\text{cm}^{-1}$ . The major absorption of glasses at different composition is summarized in Table (4). The region below 300  $\text{cm}^{-1}$  for all samples did not show any sensitivity, possibly due to excessive noise and hence this region has been excluded from the discussion. The data exhibited a water band at 3400  $\text{cm}^{-1}$ . The infrared spectra consist of a major band in the 650 - 670  $\text{cm}^{-1}$ , a shoulder at 770-790  $\text{cm}^{-1}$ , a band at 980-1000  $\text{cm}^{-1}$ , a band at 600-580  $\text{cm}^{-1}$  and a band at 480-500  $\text{cm}^{-1}$ . The absorption band at 980  $\text{cm}^{-1}$ , attributed to V=O stretching, shifted to 1000  $\text{cm}^{-1}$  with increase  $\text{V}_2\text{O}_5$  content {this data are closed with Hirashima, [15]}. The band around 480-500  $\text{cm}^{-1}$  is due to Te-O-V stretching. Absorption at 650-670  $\text{cm}^{-1}$  and shoulder at 770-790  $\text{cm}^{-1}$  both attributed to  $\text{TeO}_3$  trigonal pyramid [15] was also observed. On the other hand, absorption at 600  $\text{cm}^{-1}$  is due to the stretching vibration of  $\text{Te-O}_{\text{ax}}$  bond in the deformed  $\text{TeO}_4$  units [16]. From these results, we conclude that: infrared spectroscopies of vanadate tellurite glasses indicate the transformation of the basic structural unit of  $\text{TeO}_4$  to  $\text{TeO}_3$  with the addition of modifier.

The quantitative interpretation of the above absorption bands will be based on the experimental wavenumber of each oxide present in the glass as Table (5) and also by using the next relation

$$\nu = \frac{1}{\lambda} = \left( \frac{1}{2\pi c} \right) \sqrt{\frac{f}{\mu}} \quad (7)$$

Where  $\nu$  is a wave number in  $\text{cm}^{-1}$ ,  $c$  is the speed of light,  $f$  is the force constant of the bond, and  $\mu$  is the reduced mass of the molecule R-O and

$$\mu = \frac{(m_R m_O)}{(m_R + m_O)} \quad (8)$$

Where  $\mu$  is the reduced mass of the molecule R-O and  $m_R$ ,  $m_O$  are the atomic

weight in kg of cation  $R$  and anion  $O$  respectively.

$$f = 17 / r^3 (md\text{\AA}^{-1}) \quad (9)$$

Where  $f$  is the bending or stretching force constant and  $r$  bond length of the cation-anion. By adopting the bond length of Te-O, La- O and V-O [17] as tabulated in Table (6). Also Table (6) summarizes the calculated reduced mass of the cation-anion stretching force constant and the theoretical wavenumber by using Eq.(7). From Table (5) and Table (6) it is clear that the theoretical values are in between the experimental values of the pure oxides that used in the present binary glass systems.

#### 4- Conclusions:

The value of  $E_{opt}$  increased from (3.51 to 3.61 eV) with increasing  $La_2O_3$  content from (5 to 20 mol.%) and increased from (2.67 to 3.03 eV) with increasing  $V_2O_5$  content from (10 to 50 mol.%). The doping with  $V_2O_5$  decreased the  $E_{opt}$  of pure  $TeO_2$ , ( $E_{opt}$  of pure  $TeO_2$  =3.79eV), and can attributed to the increase of the NBO atoms, while doping with  $La_2O_3$  gave a lower concentration of NBO atoms than  $V_2O_5$ . The value of  $E_{ta}$  decrease from (0.1006 to 0.0826 eV) with increasing  $La_2O_3$  content from (5 to 20 mol%) and from (0.2085 to 0.1619 eV) with increasing  $V_2O_5$  content from (10 to 50 mol%). From these values, the widths of the band tails of the localized states are found to depend upon the kind of the modifier and they are in the range of amorphous semiconductors. From the calculations of the oxide ion average Polarizability ( $\alpha_0^{2-}$ ) and optical basicity ( $\Lambda$ ) for  $(100-x)TeO_2-(x)V_2O_5$ , where  $x$  change from (10 to 50 mol.%) by using the average electronegativity ( $\chi_{2av}$ ) it has been concluded that:

- ( $\alpha_0^{2-}$ ) are increased from ( $2.294 \times 10^{-24} \text{cm}^{-3}$  to  $2.307 \times 10^{-24} \text{cm}^{-3}$ ) with increasing  $V_2O_5$  content from (10 to 50 mol%),
- While ( $\Lambda$ ) are decreased from (0.971 to 0.96) with increasing  $V_2O_5$  content from (10 to 50 mol%).

From this results, the tellurite glass containing  $V_2O_5$  show large oxide ion polarizability between 2-3 Å can be attributed to the empty d orbital of the

**R. EL – Malawany et al .**

corresponding cation , their high coordination number towards oxide ions and relatively large cation Polarizability.

The IR spectra the ordinary band for pure  $\text{TeO}_2$  are  $640 \text{ cm}^{-1}$  shift from ( $610$  to  $670 \text{ cm}^{-1}$ ) with increasing  $\text{La}_2\text{O}_3$  content from (5 to 20 mol%) and from ( $650$  to  $670 \text{ cm}^{-1}$ ) with increasing  $\text{V}_2\text{O}_5$  content from (10 to 50 mol%). The previous qualitative description will be analyzed quantitatively according to each stretching force constant of bond  $f$ , and reduced mass of the cation-anion. We found high correlation between the obtained experimental values of wave number and calculated wave number.

**References:**

1. NTT Electronics, " Optical Fiber Modulues", [www.nel.co., JP](http://www.nel.co.jp)
2. Urbach F., Phys. Rev., 92, 1324, (1953).
3. Davis E. and Mott N., Philos. Mag., 22, 903, (1970).
4. Mott N. F. and Davis E. A., "Electronic Processes in Non-crystalline Materials", Oxford Univ. Press, (1971).
5. R.El-Mallawany, A. Abdel-Kader, M.El-Hawary and N.El-Khoshkhany, to be publishing, scientific Journal of Faculty of Science, Minufiya University.
6. Neov S., Gerassimova I., Krezhov K., Sidzhimov B. and Kozhukharov V., Phys. Status Solidi A, 47, 743, (1987).
7. Al-Ani K., Hogarth C. A. and El-Mallawany R., J. Mater. Sci., 20, 667, (1985).
8. Kim S. H., Yoko T. and Sakka S., J. Am. Ceram. Soc., 76, 4, 865, (1993).
9. Reddy R. R., Ahammed Y. N., Azeem P. A., Gopal K. R. and Rao T. V. R., J. Non-Cryst. Solids, 286, 169, (2001).
10. Dimitriev Y., Dimitrov V. and Arnaudov M., J. Mater. Sci., 18, 1353, (1983).
11. Bahgat A. A., Shaisha E. E. and Sabry A. I., J. Mater. Sci., 22, 1323, (1987).
12. Shaisha E. E. , Bahgat A. A., Sabry A. I. and Eissa N. A., Phs. Chem. Glasses 26, 91, (1985).
13. Lindqvist O., Acta Chem. Scand., 22(3), 977, (1968).
14. Arnaudov M., Dimitrov V., Dimitriev Y. and Markova L., Mater. Res. Bull., 17, 1121, (1982).



## UV-IR Spectra of the New Tellurite Glasses of ...

15. Hirashima H. and Tamura E., XVI. Int. Congr. On Glass Madrid, 4, 133, (1992).
16. Arnaudov M., Dimitrov V., Dimitriev Y. and Markova L., Mater. Res. Bull., 17, 1121, (1982).
17. Wells A. F., Structural Inorganic Chemistry 3<sup>rd</sup> p. 465 Oxford (1962).

**Table (1):**

**Optical properties of binary  $\text{TeO}_2\text{-La}_2\text{O}_3$  and  $\text{TeO}_2\text{-V}_2\text{O}_5$  glasses for different percentage of modifier in mol%.**

Glass Composition	Cut-off Wavelength (nm)	$E_{\text{opt}}$ (eV)	Constant A ( $\text{cm}^{-1}\text{eV}^{-1}$ )	$E_{\text{ta}}$ (eV)
<b><math>\text{TeO}_2\text{-La}_2\text{O}_3</math></b>				
95 - 5	335.5	3.51	5.38	0.1006
92.5 - 7.5	333	3.52	4.9	0.0987
90 - 10	331	3.54	4.825	0.0932
87.5 - 12.5	329	3.55	4.815	0.927
85 - 15	327	3.578	4.71	0.0916
82.5 - 17.5	325	3.59	4.785	0.0871
80 - 20	321	3.61	4.797	0.0826
<b><math>\text{TeO}_2\text{-V}_2\text{O}_5</math></b>				
90 - 10	413	2.67	3.039	0.2085
80 - 20	409	2.7	3.07	0.2089
75 - 25	400	2.76	2.87	0.245
70 - 30	392.5	2.79	2.84	0.2489
65 - 35	388	2.87	3.03	0.2214
60 - 40	385	2.93	3.22	0.2192
55 - 45	381	2.97	3.21	0.1801
50 - 50	377	3.03	3.38	0.1619

R. EL - Malawany et al .

**Table (2):**

Average electronegativity ( $\chi_{2av}$ ), optical basicity  $\Lambda(\chi_{2av})$ , oxide ion polarizability ( $\alpha_0^{2-}$ )( $\chi_{2av}$ ) values of binary tellurite glasses.

Glass composition	Average electronegativity ( $\chi_{2av}$ )	Electronic polarizability ( $\alpha_0^{2-}$ )( $\times 10^{-24} \text{ cm}^{-3}$ )	Optical basicity $\Lambda(\chi_{2av})$
<b>TeO<sub>2</sub>-La<sub>2</sub>O<sub>3</sub></b>			
95 - 5	2.98	2.299	0.967
92.5- 7.5	2.968	2.303	0.963
90 - 10	2.956	2.307	0.959
87.5- 12.5	2.944	2.312	0.956
85 - 15	2.933	2.315	0.952
82.5- 17.5	2.921	2.319	0.948
80 - 20	2.909	2.324	0.945
<b>TeO<sub>2</sub>-V<sub>2</sub>O<sub>5</sub></b>			
10 - 90	2.994	2.294	0.971
20 - 80	2.985	2.298	0.968
25 - 75	2.981	2.299	0.967
30 - 70	2.976	2.301	0.966
35 - 65	2.972	2.302	0.964
40 - 60	2.967	2.304	0.963
45 - 55	2.963	2.305	0.961
50 - 50	2.959	2.307	0.960

**Table (3):**

The experimental IR absorption band position for binary lanthanum tellurite glasses.

Glass Composition	$q_1$ (cm <sup>-1</sup> )	$Q_2$ (cm <sup>-1</sup> )	$q_3$ (cm <sup>-1</sup> )	$q_4$ (cm <sup>-1</sup> )
TeO <sub>2</sub> -La <sub>2</sub> O <sub>3</sub>				
95 - 5	560	580	610	740
92.5 - 7.5	560	590	630	750
90 - 10	560	595	640	760
87.5 - 12.5	580	600	650	770
85 - 15	580	610	650	770
82.5 - 17.5	590	620	655	780
80 - 20	610	630	670	785

R. EL – Malawany et al .

**Table (4):**

**The experimental IR absorption band position for  
binary vanadate tellurite glasses.**

Glass Composition	$q_1(\text{cm})^{-1}$	$q_2(\text{cm})^{-1}$	$q_3(\text{cm})^{-1}$	$q_4(\text{cm})^{-1}$	$q_5(\text{cm})^{-1}$
$\text{TeO}_2 - \text{V}_2\text{O}_5$					
90 - 10	480	600	650	770	980
80 - 20	485	600	660	780	980
75 - 25	480	600	655	785	980
70 - 30	480	595	660	760	980
65 - 35	485	590	660	780	985
60 - 40	495	585	670	790	990
55 - 45	500	580	665	790	995
50 - 50	500	580	670	790	1000

**Table ( 5):**

The IR absorption band position for pure tellurium and oxides.

Glass	$q_1(\text{cm}^{-1})$	$q_2(\text{cm}^{-1})$	$q_3(\text{cm}^{-1})$	$q_4(\text{cm}^{-1})$	$q_5(\text{cm}^{-1})$
TeO <sub>2</sub>	340		640	740	
<u>Oxide</u>					
TeO <sub>2</sub>	340		635	780	
La <sub>2</sub> O <sub>3</sub>	590		640		
V <sub>2</sub> O <sub>5</sub>	500	550	610	820	1010

**Table (6):**

The theoretical IR band position of the tellurium, lanthanum and vanadium oxides.

Cation	Atomic weight	Rest mass Of cation ( $10^{-27}\text{kgU}^{-1}$ )	Reduced mass Of catio-O ( $10^{-26}\text{kgU}^{-1}$ )	Bond Length (nm)	Stretching Force constant ( $\text{Nm}^{-1}$ )	Theoretical Wave number ( $\text{cm}^{-1}$ )
Te	127.61	211.94	2.361	1.99	215.7	507.08
La	138.91	230.73	2.383	2.517	106.6	354.83
V	50.942	84.615	2.022	1.83	277.4	621.39

R. EL - Malawany et al .

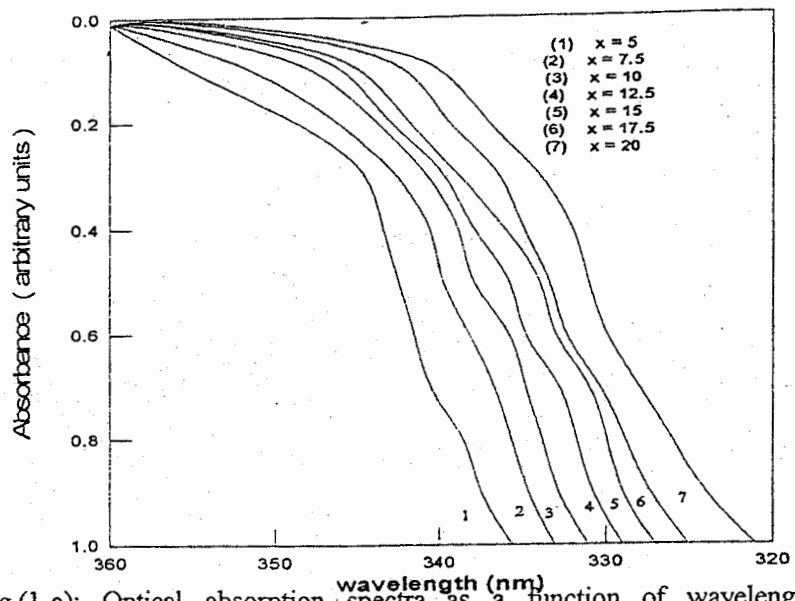


Fig.(1-a): Optical absorption spectra as a function of wavelength for  $(\text{TeO}_2)_{100-x}(\text{La}_2\text{O}_3)_x$

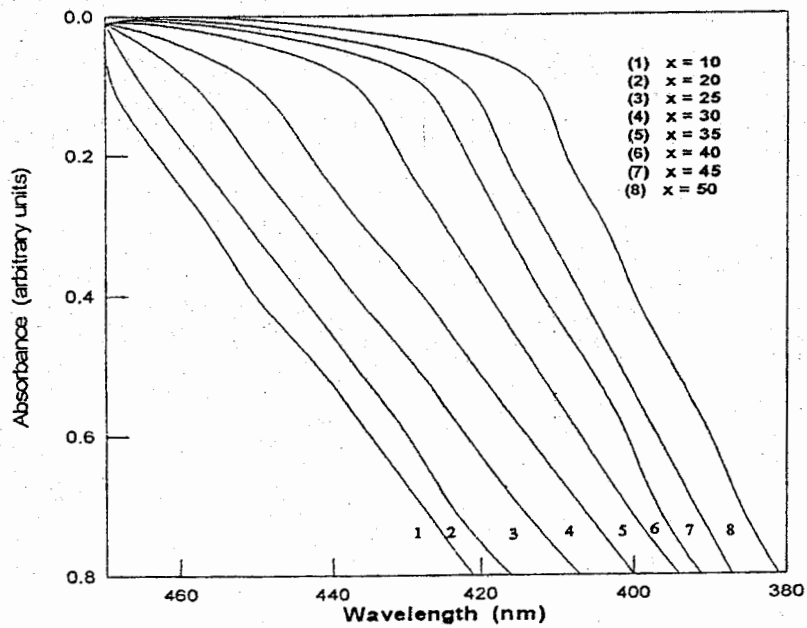


Fig.(1-b): Optical absorption spectra as a function of wavelength for  $(\text{TeO}_2)_{100-x}(\text{V}_2\text{O}_5)_x$

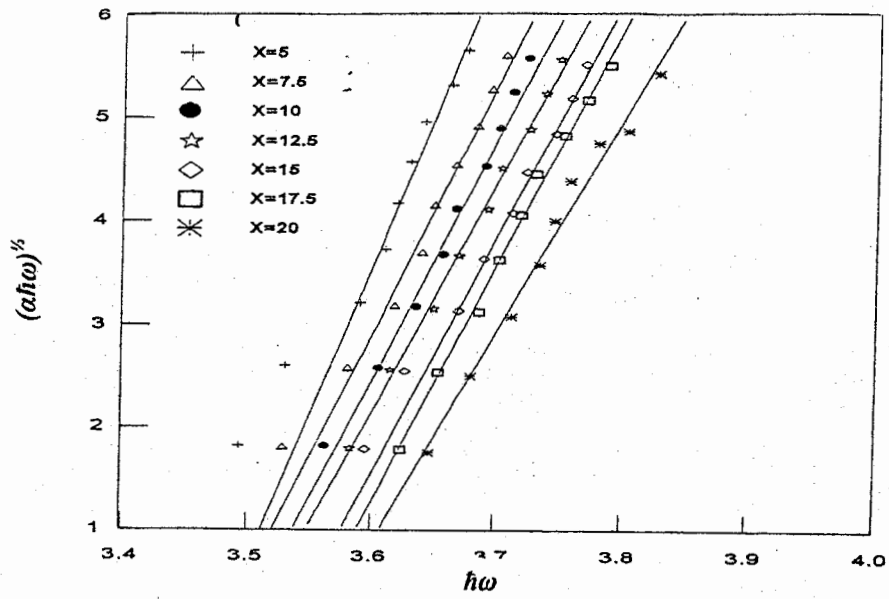


Fig.(2-a): Variation of  $(\alpha\hbar\omega)^{1/2}$  with  $(\hbar\omega)$  for the binary lanthanum tellurite glasses  $(\text{TeO}_2)_{(100-x)}-(\text{La}_2\text{O}_3)_x$

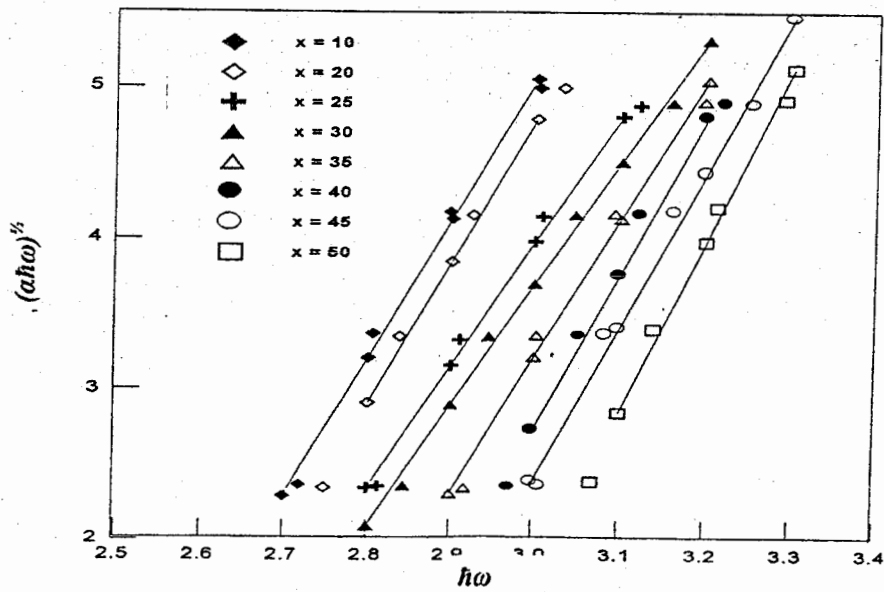


Fig.(2-b): Variation of  $(\alpha\hbar\omega)^{1/2}$  with  $(\hbar\omega)$  for the binary vanadate tellurite glasses  $(\text{TeO}_2)_{100-x}-(\text{V}_2\text{O}_5)_x$ .

R. EL - Malawany et al .

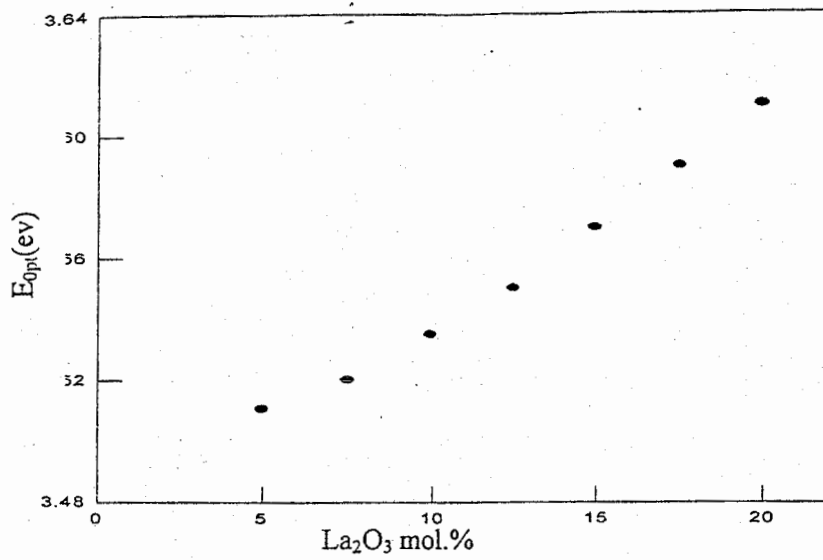


Fig. (3-a): variation of  $E_{opt}$  with ( $La_2O_3$  mol.%) for the binary lanthanum tellurite glasses  $(TeO_2)_{(100-x)}(La_2O_3)_x$ .

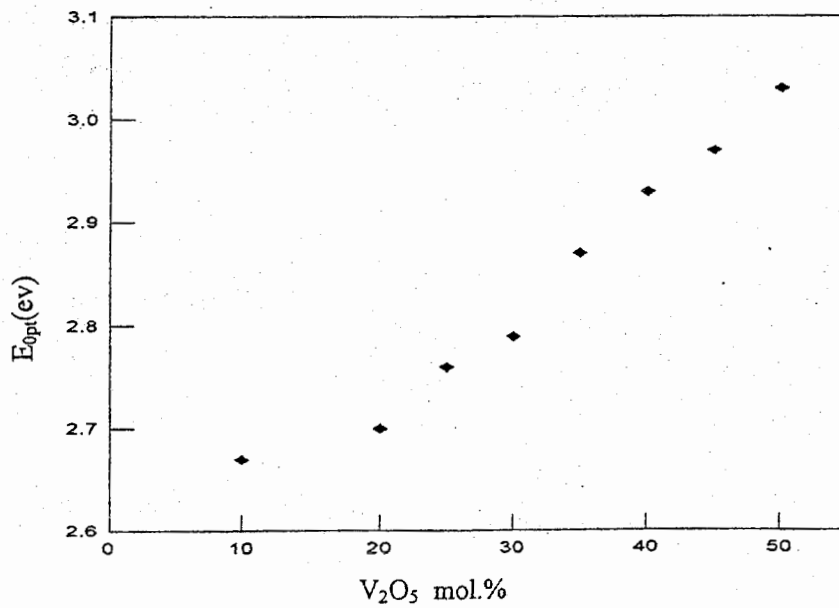


Fig. (3-b): variation of  $E_{opt}$  with ( $V_2O_5$  mol.%) for the binary vanadate tellurite glasses  $(TeO_2)_{100-x}(V_2O_5)_x$ .



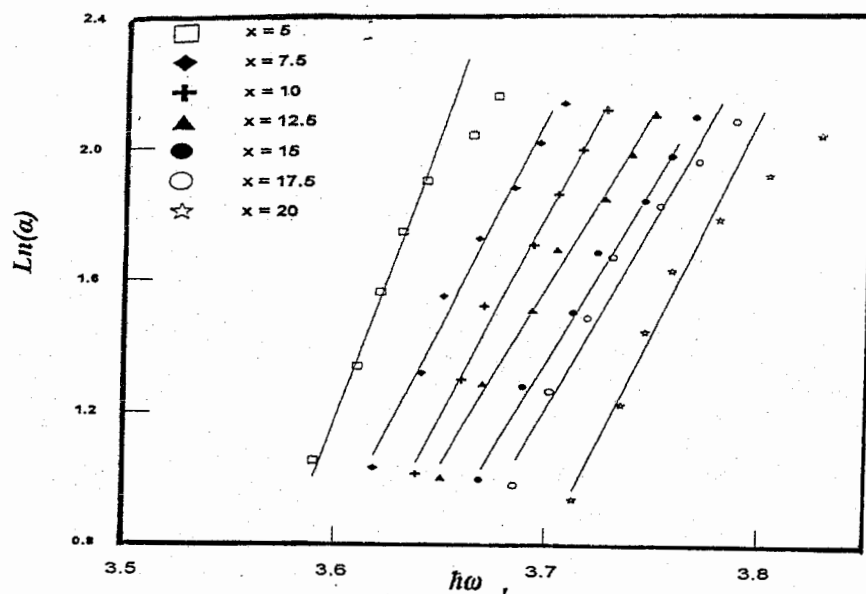


Fig.(4-a): Variation of  $\ln(\alpha)$  with  $(\hbar\omega)$  for lanthanum tellurite glasses

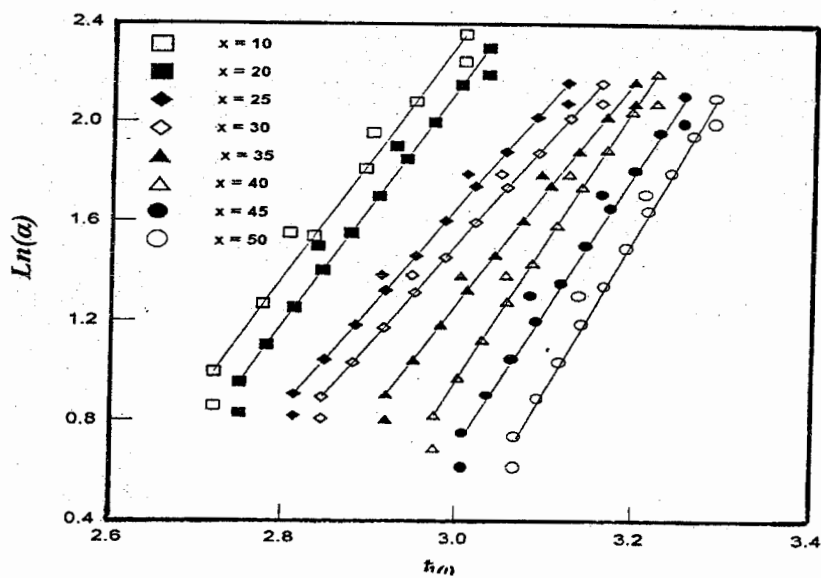
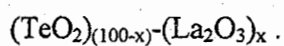
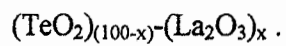


Fig.(4-b): Variation of  $\ln(\alpha)$  with  $(\hbar\omega)$  for vanadate tellurite glasses



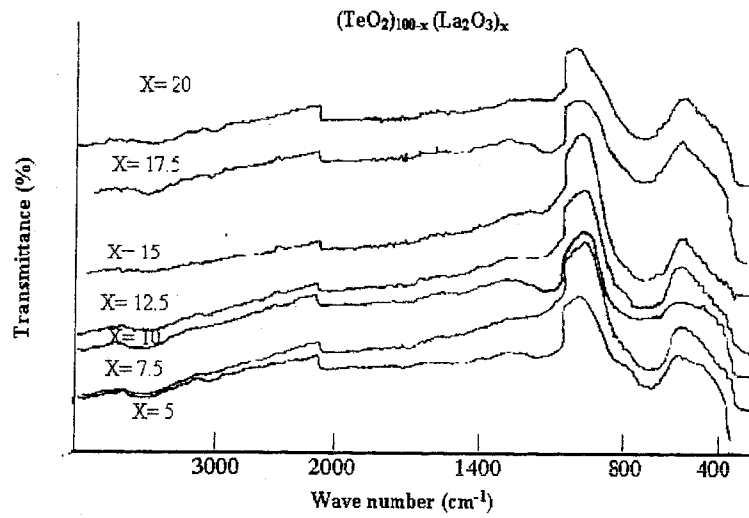


Fig. (5-a) experimental IR spectra of the binary lanthanum tellurite glasses.

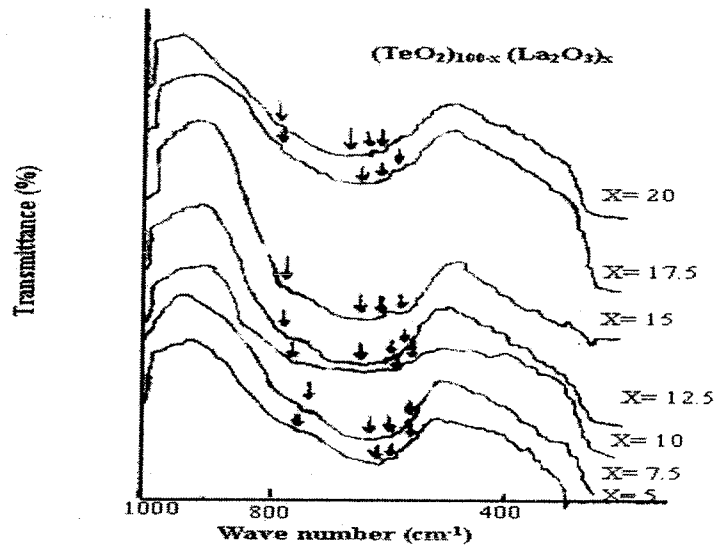


Fig. (5-b) experimental IR absorption bands of the binary lanthanum tellurite glasses in the range 200-1000  $\text{cm}^{-1}$

UV-IR Spectra of the New Tellurite Glasses of ...

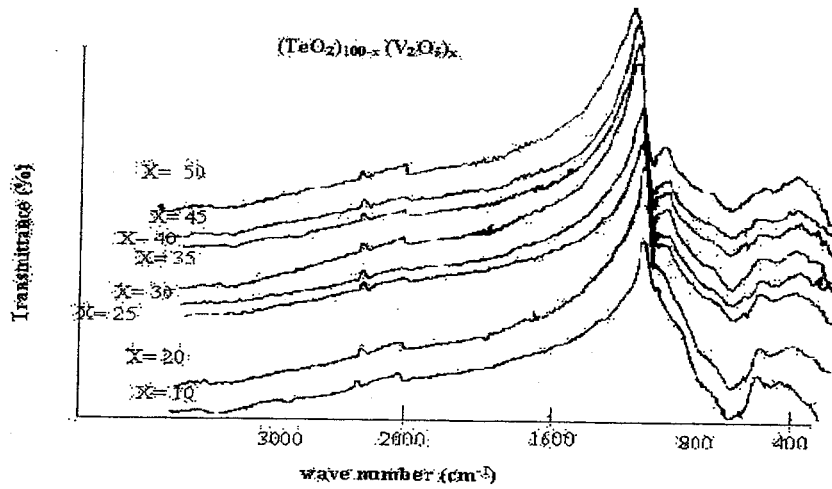


Fig. (6-a) experimental IR spectra of the binary vanadium tellurite glasses.

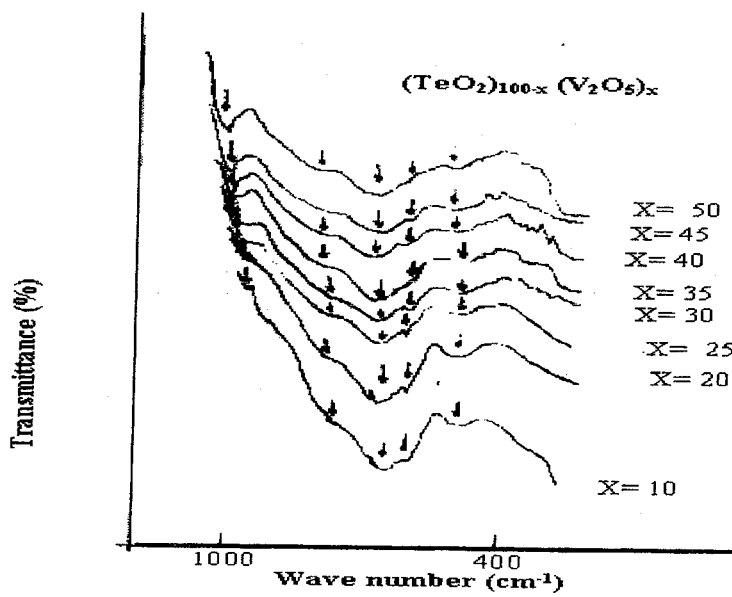


Fig. (6-b) experimental IR absorption bands of the binary vanadium tellurite glasses in the range  $200\text{-}1000\text{ cm}^{-1}$ .